IEEE Access
Multidisciplinary ⋮ Rapid Review ⋮ Open Access Journal

Received 4 June 2024, accepted 4 July 2024, date of publication 10 July 2024, date of current version 18 July 2024.

Digital Object Identifier 10.1109/ACCESS.2024.3425933

RESEARCH ARTICLE

Efficient Multiobjective Optimization Framework for Induction Heating Systems Design

ENRICO SPATERI, (Graduate Student Member, IEEE), LORENZO SABUG JR., FREDY RUIZ, (Senior Member, IEEE), AND GIAMBATTISTA GRUOSSO, (Senior Member, IEEE)
Dipartimento di Elettronica Informazione e Bioingegneria, Politecnico di Milano, 20133 Milan, Italy
Corresponding author: Giambattista Gruosso (giambattista.gruosso@polimi.it)

ABSTRACT Induction heating is an efficient alternative to fuel combustion in thermal applications. The design of the coil arrangement is a complex problem, constrained by electromagnetic and thermal dynamics. This article proposes a multi-objective optimization methodology for the geometric design of winding distribution on both the radial and the height arrangement for coils in induction heating systems around generic axisymmetric convex workpieces. A novel parametrization using the curvilinear abscissa allows for an efficient formulation for the windings distribution coordinates and avoids the use of non-linear geometric constraints in the formulation. Coil configuration problems with many degrees of freedom are solved as black-box optimization problems using the Set Membership Global Optimization method in conjunction with a finite element-based simulator. The proposed methodology is verified over several electromagnetic finite element analysis-based case studies with increasing complexity. The methodology is first tested over two target power density profiles obtained by the finite element forward problem and set over the surface of an axisymmetric convex cookware. Then, the methodology is verified with four arbitrary non-smooth power density profiles. The results show that the proposed method is suitable for solving simultaneous design optimization problems in induction heating systems, improving the optimization complexity capability.

INDEX TERMS Black-box optimization, induction heating, coil design, winding distribution, multi-objective optimization.

I. INTRODUCTION

In many industrial and domestic applications, induction heating (IH) [1] has proven to be a more sustainable alternative to fuel combustion due to its highest efficiency without exhaust greenhouse gas emissions. In the interest of improving the efficiency and heat transfer performance, optimizing the coil arrangement is still an open problem, in conjunction with the design of the electromagnetic subsystem, the power converter, and the regulation strategy. The coil arrangement (otherwise referred to as ''winding distribution'') problem has been considered in different settings, utilizing different optimization methodologies, objective functions designs, and model parametrizations [2], [3], [4], [5], [6].

The associate editor coordinating the review of this manuscript and approving it for publication was Bijoy Chand Chatterjee.

Most previous works on winding distribution optimization are limited to a few degrees of freedom and consider simple workpiece geometries as shown in Fig. 1, resulting in a restricted flexibility in the design. For example, [7], [8], [9] considered the optimization of the thermal and power distribution, tuning the orthogonal distances between a horizontal plate and each winding, as in Fig. 1(a). In works like [2], [4], [5], [8], [10], and [11], genetic and bio-inspired multi-objective algorithms were tested on a two-dimensional axisymmetric problem to achieve field uniformity and coil mass reduction in a setting like the one in Fig. 1(b).

This coil arrangement optimization problem has also been proposed for testing numerical methods for electromagnetics. The Testing Electromagnetic Analysis Methods (TEAM) problems [12] were developed to test the first generation of electromagnetic numerical methods and optimization

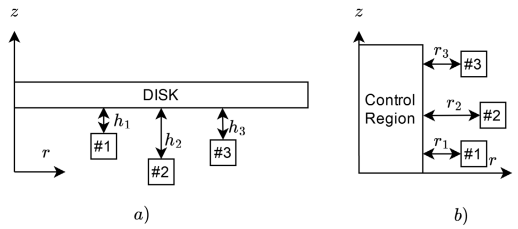

FIGURE 1. Geometries analyzed in previous optimization problems. In (a) the coil is optimized to obtain a desired power generated over the surface of a plate, in (b) the coil is optimized to generate an homogeneous magnetic field.

algorithms, as in TEAM 35. More recently, [6] has proposed a relevant testing benchmark for the arrangement of coil geometry to challenge advanced numerical methods and the latest multi-objective optimization algorithms.

To the best of our knowledge, no previous works deal with winding distribution design on both the radial and the height arrangements. Coil optimization with two degrees of freedom can open new usage possibilities for IH systems for a broader range of industrial applications, including those enabled by new technologies such as additive manufacturing. In [13], the author proposes employing additive manufacturing technology to print IH coils. This facilitates the production of coils with complex shapes tailored for those demanding applications that require precise tuning of the power profile generated on the workpiece surface. Moreover, Higher degrees of freedom for the coil design can lead to improved heating performance and better efficiency for workpieces with complex shapes. However, the increment in the problem dimensionality leads to more challenging design processes.

Various practical requirements constrain the design process of an IH system, and different criteria are employed to evaluate the quality of a solution. Thus, the design is often formulated as a multi-objective optimization problem. In general, designing a complete IH system requires the simultaneous choice of the coil arrangement, the converter topology, and its power electronics components [14]. IH systems are typically evaluated according to two performance indices: the thermal performance and the safe operative working region of the resonant converter. The thermal performance of the IH system is described by the superficial power distribution generated on the heated material. While in some applications, it is required that the electro-thermal system heats the workpiece to a target temperature profile [15].

Due to their complexity, the behavior of IH systems is mainly simulated via numerical methods rather than obtained through analytical equations, [16], [17]. For IH system optimization, finite-element method (FEM)-based simulations are commonly used to evaluate the performance indices of a design. FEM simulations are considered black-box models since it is not possible to derive closed-form mathematical expressions relating to the coil geometry and the resulting magnetic fields and power distributions. Hence, data-driven global optimizers are more appropriate tools for solving this kind of design problem than model-based ones. However, global optimizers based on black-box models can require a long time to achieve convergence. Evaluating the cost function in gradient-based optimization techniques can result in very long simulation times and hardware-consuming procedures and can require some *a priori* information as the objective function convexity for a reliable algorithm convergence. On the other hand, population- or generation-based algorithms such as particle swarm optimization (PSO) [18], [19] or genetic algorithms (GA) require many function evaluations to reach convergence and can be prohibitively complex for high-dimensional problems. Finally, the recently proposed Set Membership Global Optimization (SMGO) method [20], [21] is a promising data-driven optimizer due to its competitive iteration-based optimization performance compared to the *de facto* standard Bayesian optimization (BO) solutions. Furthermore, SMGO features a light computational burden, allowing it to be used for problems with more optimization variables, which are impractical for other approaches.

This paper proposes an optimization methodology for designing the coil geometric configuration in IH applications, considering both the radial and height dimensions as optimization variables. A novel coil coordinate system parametrization allows for better constraint management, avoiding spatial overlapping among windings. Moreover, the proposed parametrization is generalizable to any convex heating surface, allowing the optimization of coil configurations even for complex-shaped workpieces. The design problem is based on stationary frequency-domain electromagnetic finite element simulations. Each simulation provides the performance values for an individual design configuration. Furthermore, the advantages of the SMGO method are exploited to efficiently solve the resulting high-dimensional black-box optimization problem of arranging the windings around convex-shaped 2D geometries to achieve a target power profile on the workpiece surface. The proposed methodology is evaluated on multiple case studies that include a mix between the test-benches proposed in [3] and [6]. The results of the power profile optimization problems highlight that the introduced parametrization, in conjunction with SMGO, results in excellent performances even for design problems with a high number of coils. Moreover, a Pareto front analysis, trading-off power profile accuracy, and equivalent inductance values illustrates the method's capabilities for simultaneously designing induction heating industrial solutions considering converter compatibility and heating performance for electromagnetic problems.

The paper is organized into 5 sections. The design problem, IH physical principles, and the proposed parametrization are introduced in Section II. Section III presents a summary of the SMGO algorithm and discusses the implementation of the optimization setup. Case studies on several representative IH system design problems are shown in Section IV, and the conclusions are drawn in Section V.

II. PROBLEM FORMULATION

The design problem considers an axisymmetrical IH system as illustrated in Fig. 2. The IH system contains a generic workpiece with convex surface, heated by an external solenoid coil with N_w windings. The windings are supplied in series with an ac current $\vec{I}_0$ of fixed frequency f. The position of each coil winding is defined by two degrees of freedom: the radius r measured from the axis of symmetry, and the height z. Thus, the design problem has $2N_w$ tunable variables, and the optimization variable can be defined in this coordinate system as

$$\boldsymbol{x}_+ \doteq [\underbrace{r_1, z_1,}_{\text{first winding}} \quad r_2, z_2, \ldots, \quad \underbrace{r_{N_w}, z_{N_w}}_{N_w\text{-th winding}} \ ].$$

The design process aims to achieve proper heating of the workpiece, with high efficiency and robustness. To achieve this, the leading performance indicator is the power distribution generated on the workpiece surface. However, it is not the only index that measures the system's quality. From the supply side, the equivalent lumped-circuit parameters of the coil-workpiece couple are fundamental to determine the performance of the power converter in terms of operating frequency, conversion efficiency, and required ratings for the components, among others.

A. COORDINATE SYSTEMS PARAMETRIZATION

In axisymmetric systems, the position for the i-th winding is expressed in Cartesian coordinates as $\{r_i, z_i\}$. Such coordinates are intuitive for simple problems where the system geometry is arranged along the r-axis [3] or the z-axis [4], and the windings are optimized along the direction normal to the workpiece surface, as in Fig. 1. In these cases, the tangential positions of all the windings are fixed and a constant distance between the windings is usually maintained. When the windings are free to move in the whole space, two or more windings can overlap due to their finite radius R_c. Therefore, we need to ensure that the following constraint is satisfied:

$$\sqrt{(r_i - r_j)^2 + (z_i - z_j)^2} \geq 2R_c \quad \forall i, j \quad i \neq j. \tag{1}$$

The constraint in (1) is non-linear, and in cases with more coils, difficult to enforce. Therefore, in this paper, we propose a new parametrization of the optimization variables as a function of a curvilinear abscissa defined on the heated surface, mapping the points of a curve in the Cartesian workframe with an incremental quantity s. This variable is the tangential component of the curvilinear abscissa and its maximum value corresponds to the length L of the curve:

$$0 < |s| < L$$

A unique value of s can identify each point along the red curve in Fig. 2. Furthermore, the second coordinate n denotes the normal direction from the curvilinear abscissa. Thus, if the surface is convex, each couple (n, s) corresponds to a unique

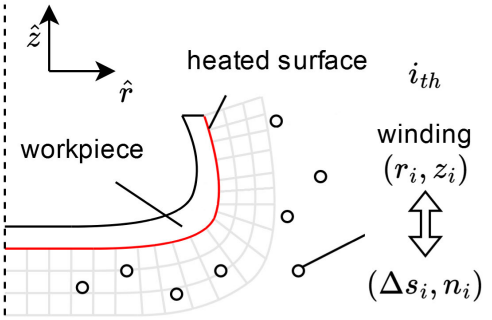

FIGURE 2. Axisymmetric geometry and the representation of the incremental curvilinear abscissa parametrization. If the red heated surface is convex, each point in the grey grid (n, s) corresponds to a unique point in the Cartesian coordinates.

Cartesian point (r, z), and the following transformation (or mapping) is bijective:

$$(r_w, z_w) = g(n, s) \tag{2}$$

In addition to the coordinates trasformation, we introduce an incremental parametrization that relates the tangential components of consecutive windings s_i and s_{i-1}:

$$\Delta s_i = s_i - s_{i-1} \tag{3}$$

The tangential component for the first winding is defined as its absolute value s_1.

The final transformation for the new parametrization is defined as follows:

$$\boldsymbol{x}_+ \doteq \left[r_1, z_1, r_2, z_2, \ldots r_{N_w}, z_{N_w}\right]$$
$$\Updownarrow$$
$$\boldsymbol{x} \doteq \left[n_1, s_1, n_2, \Delta s_2, \ldots, n_{N_w}, \Delta s_{N_w}\right]$$

In the new parametrization, the spacing between coils is imposed by simple decoupled constraints of the form

$$\Delta s_i \geq 2R_c \quad \forall i. \tag{4}$$

B. IH PHYSICAL SYSTEM DESCRIPTION

Given a coil configuration $\boldsymbol{x}_+$, the performance of the IH system is determined by its resulting electromagnetic and thermal behavior. An electromagnetic finite element simulation is exploited to analyze the IH system in the frequency domain.

The Maxwell and thermodynamic equations describe the physical behavior of IH systems. Given a geometric configuration and an excitation current, the electromagnetic results can be obtained by solving the following partial differential equation (expressed in Cartesian coordinates):

$$\vec{\nabla} \times (\nu(|\vec{H}|)\vec{\nabla} \times \vec{A}) - \vec{I}_0(\boldsymbol{x}_+) - \sigma \frac{d\vec{A}}{dt} = 0 \tag{5}$$

where $\nu(|\vec{H}|)$ is the inverse of the permeability, σ is the workpiece electrical conductivity, $\vec{I}_0(\boldsymbol{x}_+)$ is the current density prescribed in the windings positioned at $\boldsymbol{x}_+$ and $\vec{A}$ is the resulting magnetic potential. The heating on the workpiece is

produced by the Ohmic losses generated by the eddy currents induced inside the ferromagnetic conductive material and described by the Lenz's law. Both the eddy current density and the heat power density $P(\boldsymbol{x}_+)$ exponentially decay along the material depth according to the skin depth value $\delta = 1/\sqrt{\pi\sigma\omega\mu_0\mu_r}$, causing the most of the heat power to be generated on the workpiece surface.

We consider two important performance indices for the evaluation of the IH system. The first pertains to the spatial heat density profile on the workpiece, measured as its deviation from a given target profile. The second is the value of the equivalent lumped-circuit coil inductance $L_{eq}(I, f)$, estimated at a given current I and frequency f. Note that the combined design of alternative parameters, such as Q-factor, operation frequency, and efficiency are related or directly dependent on the equivalent inductance value [14].

C. OPTIMIZATION PROBLEM

During the design phase the power profile in the IH system is managed by changing the coil arrangement around the workpiece. Each winding has radius R_c and the system is closed inside a semicircular region of radius R_{out}.

The coil design problem is defined as the optimization problem:

$$\boldsymbol{x}^* = \underset{\boldsymbol{x}\in\mathbb{X}}{\operatorname{argmin}}\, J(\boldsymbol{x}) \tag{6}$$

That is, finding the optimal winding coordinates $\boldsymbol{x}^*$ (working on the proposed curvilinear abscissa coordinates), that minimizes the cost function $J(\boldsymbol{x})$.

A generic objective function can be defined as the L_n norm of any performance indicator, as follows:

$$J(x) = \left\| \hat{h} - h(\boldsymbol{x}) \right\|_{L_n} \tag{7}$$

where $\hat{h}$ is the target value and $h(\cdot)$ can be a single scalar value such as an equivalent lumped parameter of the coil-workpiece pair, a finite set of scalar values such as the heating power at a grid or list of control points on the workpiece surface; or a vector field describing the superficial distribution of a variable of interest, for example of the induced field.

Thanks to our proposed curvilinear abscissa-based parametrization, for an IH system with N_w windings, the search space of the optimization problem $\mathbb{X} \subset \mathbb{R}^D$, with dimensionality $D = 2N_w$, is defined by the following set of constraints:

$$\mathbb{X} = \begin{cases} 2R_c < s_1 < \dfrac{L}{N_w} & \\ 2R_c < \Delta s_i < \dfrac{L}{N_w} & \forall i \in 2, \ldots, N_w, \\ R_c < n_i < \overline{T} & \forall i \in 1, \ldots, N_w, \end{cases} \tag{8}$$

where L is the length of the surface and $\overline{T}$ is the maximum distance between the workpiece surface and the winding.

We now define two possible objective functions that can be employed in (6), to define the desired behavior of the IH system.

Power density profile optimization: In this case the objective function is defined as:

$$J(\boldsymbol{x}) = \left\| \breve{P}(s) - P(s, \boldsymbol{x}) \right\|_{L_2} \tag{9}$$

where $\breve{P}(s)$ is the desired power density profile along the workpiece surface coordinate. It is a one-dimensional function of the curvilinear abscissa s. Two case studies about power profile optimization are presented in subsections IV-A and IV-B.

Multi-objective optimization: A bi-objective optimization problem can be set up, for example, by adding a target on the equivalent lumped-circuit inductance $\breve{L}_{eq}$ to the cost function in (9), that is:

$$J(\boldsymbol{x}) = \left\| \breve{P}(s) - P(s, \boldsymbol{x}) \right\|_{L2} + w_l \left| \breve{L}_{eq} - L_{eq}(\boldsymbol{x}) \right| \tag{10}$$

where w_l is a weighting term. A problem of this type is presented in subsection IV-D.

III. PROPOSED BLACK-BOX OPTIMIZATION-BASED METHODOLOGY FOR IH SYSTEM DESIGN

The design problems (9) and (10), formulated in the previous section are non-linear, non-convex optimization problems, where it is not possible to derive analytic expressions of the cost functions and the performance of any set of decision variables is evaluated by computationally-intensive simulation. This condition makes it inefficient to rely on gradient-based optimizes to find (sub)optimal solutions. Hence, in this work we resort to a zeroth-order optimization algorithm to address these practical constraints. We use the Set Membership Global Optimization (SMGO) method to solve (6). In this section, we provide an brief overview of SMGO. More details and theoretical properties can be consulted in [21].

A. SET MEMBERSHIP GLOBAL OPTIMIZATION (SMGO)

SMGO is an iterative algorithm that adaptively chooses, given an existing data set, the next sampling point (in this case, the next coil configuration) to solve (6). The main assumption in SMGO is that the objective J is Lipschitz continuous, i.e.,

$$|J(\boldsymbol{x}_1) - J(\boldsymbol{x}_2)| \leq \gamma \left\| \boldsymbol{x}_1 - \boldsymbol{x}_2 \right\|, \boldsymbol{x}_1, \boldsymbol{x}_2 \in \mathbb{X},$$

with an *a priori* unknown but finite Lipschitz constant γ.

In the iterative procedure of SMGO we consider a new incoming sample, at iteration n, in the form of a tuple $\boldsymbol{x}^{(n)} \doteq \left(\boldsymbol{x}^{(n)}, z^{(n)}\right)$. In each tuple, $\boldsymbol{x}^{(n)}$ is the evaluated point (i.e., the tested coil configuration), and $z^{(n)}$ is the resulting (possibly noise-corrupted) value returned by the FEM simulation, i.e.,

$$z^{(n)} = J(\boldsymbol{x}^{(n)}) + \epsilon^{\langle n \rangle}, \left| \epsilon^{\langle n \rangle} \right| \leq \overline{\epsilon} < \infty,$$

with $\overline{\epsilon}$ being the *a priori* unknown but finite noise bound. We use $\boldsymbol{x}^{(n)}$ to iteratively build an updated data set of samples, $\boldsymbol{X}^{\langle n \rangle} = \boldsymbol{X}^{\langle n-1 \rangle} \cup \boldsymbol{x}^{(n)}$.

At iteration n we have a data set composed of n samples

$$\boldsymbol{X}^{\langle n \rangle} \doteq \left\{ (\boldsymbol{x}^{(1)}, z^{(1)}), (\boldsymbol{x}^{(2)}, z^{(2)}), \ldots, (\boldsymbol{x}^{(n)}, z^{(n)}) \right\},$$

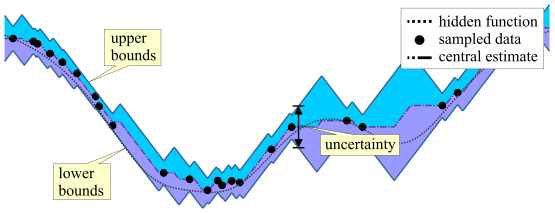

FIGURE 3. Example of Set Membership surrogate model and bounds from a sample data set.

which, together with the Lipschitz assumption, can be used to build a Set Membership (SM)-based surrogate model of the hidden function $J(\boldsymbol{x})$, as discussed next.

Note that the superscript $\cdot^{\langle n \rangle}$ denotes a quantity or object that generally changes with n, while $\cdot^{(i)}$ denotes the i-th member of a collection.

Given an estimated noise bound $\tilde{\epsilon}^{\langle n \rangle}$ and Lipschitz constant estimate $\tilde{\gamma}^{\langle n \rangle}$ (the estimation methods are discussed in [21]), the SM model provides an upper bound $\overline{J}^{\langle n \rangle}(\boldsymbol{x})$, and a lower bound $\underline{J}^{\langle n \rangle}(\boldsymbol{x})$ on the cost function, as follows

$$\overline{J}^{\langle n \rangle}(\boldsymbol{x}) = \min_{\boldsymbol{x}^{(i)} \in \boldsymbol{X}^{\langle n \rangle}} \left(z^{(i)} + \tilde{\epsilon}^{\langle n \rangle} + \tilde{\gamma}^{\langle n \rangle} \|\boldsymbol{x} - \boldsymbol{x}^{(i)}\| \right), \tag{11}$$

$$\underline{J}^{\langle n \rangle}(\boldsymbol{x}) = \max_{\boldsymbol{x}^{(i)} \in \boldsymbol{X}^{\langle n \rangle}} \left(z^{(i)} - \tilde{\epsilon}^{\langle n \rangle} - \tilde{\gamma}^{\langle n \rangle} \|\boldsymbol{x} - \boldsymbol{x}^{(i)}\| \right). \tag{12}$$

Such bounds quantify the tightest bounds on J given the existing data set $\boldsymbol{X}^{\langle n \rangle}$. Furthermore, we can quantify the central estimate $\tilde{J}^{\langle n \rangle}(\boldsymbol{x}) \doteq \frac{1}{2}\left(\overline{J}^{\langle n \rangle}(\boldsymbol{x}) + \underline{J}^{\langle n \rangle}(\boldsymbol{x})\right)$, and the uncertainty $\lambda^{\langle n \rangle}(\boldsymbol{x}) \doteq \overline{J}^{\langle n \rangle}(\boldsymbol{x}) - \underline{J}^{\langle n \rangle}(\boldsymbol{x})$ of the surrogate for any value of the decision vector $\boldsymbol{x}$. An illustration of the SM-based model is shown in Fig. 3.

The next sampling point $\boldsymbol{x}^{(n+1)}$ is selected form a set of candidate points $\boldsymbol{E}^{\langle n \rangle}$ using exploitation and exploration routines. $\boldsymbol{E}^{\langle n \rangle}$ is strategically generated following a deterministic procedure based on the history of previously sampled points $\boldsymbol{x}^{(i)} \in \boldsymbol{X}^{\langle n \rangle}$, to ensure the repeatability of any SMGO optimization run. More information regarding the generation of candidate points is available in [21].

Once the surrogate model has been updated with the new sample, SMGO attempts to execute an exploitation routine. For this, we identify the best sample at iteration n,

$$(\boldsymbol{x}^{*\langle n \rangle}, z^{*\langle n \rangle}) = \operatorname*{argmin}_{(\boldsymbol{x}^{(i)}, z^{(i)}) \in \boldsymbol{X}^{\langle n \rangle}} z^{(i)}. \tag{13}$$

And then, the exploitation candidate point $\boldsymbol{x}_\theta^{\langle n \rangle}$ is selected within a trust region $\mathcal{T}^{\langle n \rangle}$ around $\boldsymbol{x}^{*\langle n \rangle}$ as the minimizer of the exploitation metric, i.e.,

$$\boldsymbol{x}_\theta^{\langle n \rangle} = \operatorname*{argmin}_{\boldsymbol{x} \in \boldsymbol{E}^{\langle n \rangle} \cap \mathcal{T}^{\langle n \rangle}} \underline{J}^{\langle n \rangle}(\boldsymbol{x}) + \beta \tilde{J}^{\langle n \rangle}(\boldsymbol{x}). \tag{14}$$

The exploitation metric is formed as a linear combination (with default value $\beta = 0.1$) of the lower bound and the central estimate of the cost function. The exploitation candidate point $\boldsymbol{x}_\theta^{\langle n \rangle}$ is then subjected to an expected improvement test, in which the condition

$$\underline{J}^{\langle n \rangle}(\boldsymbol{x}_\theta^{\langle n \rangle}) \leq z^{*\langle n \rangle} - \eta \tag{15}$$

must be satisfied so that $\boldsymbol{x}^{(n+1)} \leftarrow \boldsymbol{x}_\theta^{\langle n \rangle}$, being η the expected improvement threshold. If such a test fails, the algorithm instead resorts to an exploration routine to select the next sampling point $\boldsymbol{x}^{(n+1)}$.

The SMGO exploration routine is designed to sample points around the search space with high uncertainty, thereby discovering the shape of the hidden function J. Using the set $\boldsymbol{X}^{\langle n \rangle}$ of candidate points generated so far, we choose the exploration point as

$$\boldsymbol{x}_\phi^{\langle n \rangle} = \operatorname*{argmax}_{\boldsymbol{x} \in \boldsymbol{E}^{\langle n \rangle}} \lambda^{\langle n \rangle}(\boldsymbol{x}) + \kappa \tau^{\langle n \rangle}(\boldsymbol{x}), \tag{16}$$

with $\tau^{\langle n \rangle}(\boldsymbol{x})$ being the age of the candidate point, which is the number of iterations from its generation up to the current iteration n, and κ a small costant parameter. While the first term in (16) prioritizes points with higher uncertainty, the second term is a slowly growing age-based term that ensures the convergence of SMGO to a global minimum, see [21] for more details. The chosen point in exploration is then directly assigned as the next sampling point, $\boldsymbol{x}^{(n+1)} \leftarrow \boldsymbol{x}_\phi^{\langle n \rangle}$.

Remark 1: The usage of a black-box optimization technique, such as SMGO, is motivated by the fact that the objective function and the operational constraints lack a closed-form expressions with respect to the coil shape. Indeed, the fitness of any particular coil configuration can only be evaluated by running finite element simulations, which are computationally expensive. To address this, the SMGO strategy iteratively updates surrogate models of the objective and constraints from the observed data, allowing a computationally cheap way to decide the next design configuration to test without estimating gradients and Hessians or randomly exploring the design space. For these reasons, SMGO is preferred over more standard gradient-based or population-based optimization strategies.

Remark 2: The use of SMGO for the IH design optimization problem goes hand-in-hand with the proposed parametrization discussed in Section III. The Lipschitz continuity assumption of the underlying function J throughout the search space $\mathbb{X}$ is not a strong requirement in this context. It must be guaranteed that a valid and finite value z is obtained from the FEM simulation for any tested $\boldsymbol{x} \in \mathbb{X}$. Note that the dependence of the magnetic flux on the coil geometry is defined by the Maxwell PDE in (5). Then, the variation of any performance indicator derived from the magnetic potential, given a bounded modification of the winding positions, must be bounded by a finite constant. No jumps can be observed in the solutions of the PDE as the coil positions defined by the decision variables are varied continuously and smoothly. Moreover, in the Cartesian coordinates-based parametrization, coil overlapping can occur which leads to simulation failure, i.e., the simulation does not start due to invalid input, and no numerical value for z is acquired for the

tested point. On the other hand, the incremental curvilinear abscissa parametrization avoids such overlapping scenarios, resulting in a simply connected and compact space $\mathbb{X}$ for the decision variables. The evaluation results are valid for all $\boldsymbol{x} \in \mathbb{X}$, and the Lipschitz continuity of J is always ensured.

B. IMPLEMENTATION SETUP

SMGO is interfaced with COMSOL AC/DC module [22], which evaluates each test point $\boldsymbol{x}^{(n)}$ via magnetic-fields FEM simulation. Each $\boldsymbol{x}^{(n)}$ in the curvilinear abscissa parametrization (see Section II) is converted to the axisymmetric coordinates compatible with COMSOL. The physical equations and interactions are conveniently managed in the simulation software. For the material B-H characteristic, the frequency domain simulation uses an average effective B-H curve [23]. Moreover, a boundary layer mesh is set on the heated surface to improve the result quality. SMGO, together with the simulations in COMSOL, are run in a machine with Intel Core i9-11900 (5.0 GHz) processor and 32 GB RAM. The average per iteration time is found to be around 6 s. The computational time is highly dominated by the FEM simulation time, while the SMGO algorithm execution requires less than 100ms to generate the successive test point.

C. ON THE OBJECTIVE CONVEXITY PROPERTIES

Due to the lack of a closed-form expression relating $\boldsymbol{x}$ to J (J values are revealed via simulation at discrete points $\boldsymbol{x}$), it is difficult to formally verify the non-convexity of (9). For the same reason, it is difficult to verify the presence of a single or multiple local and/or global minima within the considered search space. However, we perform a simple test to verify the non-convexity of J.

Let us consider a problem involving three windings ($D = 6$) for simplicity. We generate a sample windings configuration $\check{\boldsymbol{x}}$, and obtain the resulting heating power profile $\check{P}(s)$ through FEM simulations. This profile is set as the target power distribution in (6) with objective (9). We now have an optimization problem with an *a priori* known $\boldsymbol{x}^*$. That is, we know for certain that $\check{\boldsymbol{x}}$ is the global minimizer $\boldsymbol{x}^*$ (or at least, one of several) because $\check{P}(s)$ was directly generated from $\check{\boldsymbol{x}}$.

A set of randomly-generated winding configurations $\{\boldsymbol{x}_{r,i} \in \mathbb{X} : i = 1, \ldots, 100\}$ is generated. We then evaluate the cost function J along the convex combination of $\check{\boldsymbol{x}}$ and each one such $\boldsymbol{x}_{r,i}$, i.e.,

$$J_m(w) \doteq J(\check{\boldsymbol{x}} + w\,(\boldsymbol{x}_{r,i} - \check{\boldsymbol{x}})) \tag{17}$$

with $w \in [0, 1]$. A non-convex behavior is highlighted in the presence of a local minimum (or saddle region) of $J_m(w)$ along w. The same method is repeated for the rest of the test points, 23 of which presented a similar non-convex behavior. This confirms the non-convexity of J, highlighting the difficulty of the currently-considered winding optimization problem. For instance, gradient descent-based methods cannot guarantee the convergence to a global optimum for J.

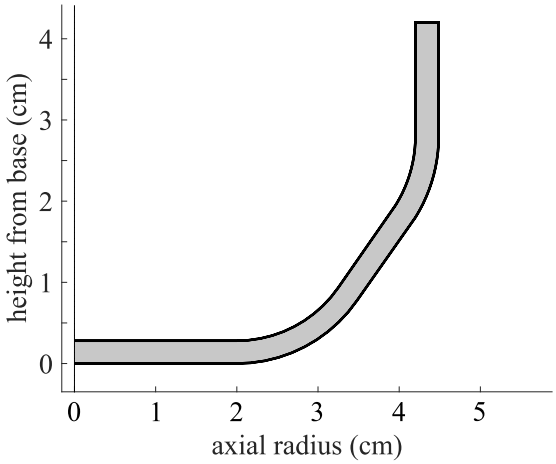

FIGURE 4. Workpiece geometry considered in the case studies.

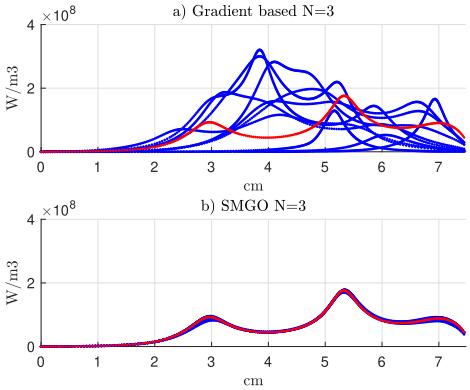

FIGURE 5. Solutions proposed by GB algorithm and SMGO from 10 independent optimization runs with random starting guesses (three windings, $N_w = 6$).

IV. CASE STUDIES

The methodology proposed in Section III is applied in two IH system design problems, involving the placement of three ($D = 6$) and eight ($D = 16$) windings, respectively. For both problems, we consider the workpiece geometry shown in Fig. 4.

A. DESIGN WITH THREE WINDINGS

The proposed method is evaluated on a low-dimensional problem related to the positioning of three coils ($D = 6$), to achieve a desired power density $\check{P}(s)$ on the workpiece surface. We validate the SMGO-based design by having it applying it to a problem with an *a priori* known solution. To start, we have a human expert to design a coil distribution $\check{\boldsymbol{x}}$, which is then used to simulate the workpiece. The power density profile obtained in the COMSOL simulation then serves as target profile $\check{P}(s)$ for the optimization. This ensures that a feasible solution exists to achieve the desired $\check{P}(s)$, with $\boldsymbol{x}^* = \check{\boldsymbol{x}}$.

The performance of SMGO is compared to that of the commonly used gradient-based (GB) algorithm. The MATLAB built-in function `fmincon` is used as the GB implementation using the same formulation of the optimization problem

TABLE 1. Power profile RMS error statistics from solutions to 10 independent optimization runs, with $N_W = 3$.

ine	GB	SMGO
ine Mean	6.918E7	2.500E6
ine Max	8.503E7	4.033E6
ine Min	4.258E7	4.210E5
ine		

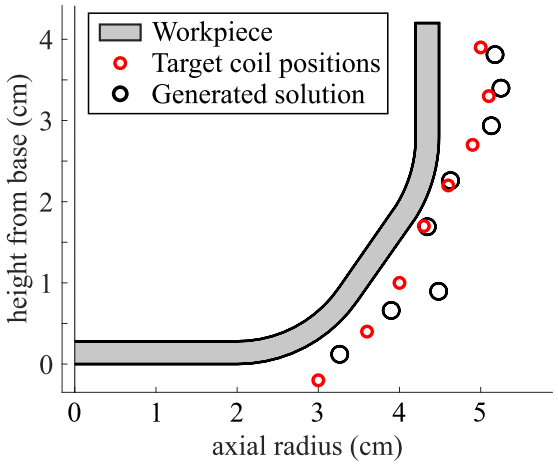

FIGURE 6. Best arrangement from SMGO compared with the target coil configuration.

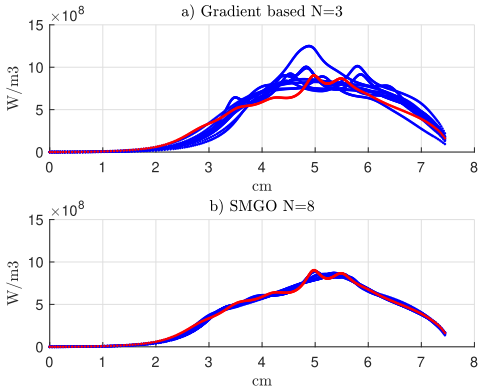

FIGURE 7. Solutions proposed by GB (a) and SMGO (b) algorithm from 8 independent optimization runs with random starting guesses (eight windings, $N_W = 16$).

TABLE 2. Power profile RMS error statistics from solutions to 8 independent optimization runs, with $N_W = 8$.

ine	GB	SMGO
ine Mean	1.156E8	3.170E7
ine Max	2.128E8	3.668E7
ine Min	7.599E7	2.118E7
ine		

described in Section II. Both methods have been executed in 10 independent runs for the same target power profile, each with an evaluation (FEM simulation) budget of $N = 1500$. Each run starts with a randomly generated starting winding configuration (serving as ''initial guess''). However, to maintain fairness in comparison, each run of both SMGO and GB starts from the same initial guess. Other commonly used global methods, such as genetic algorithms and particle swarm optimization have been also tested, but due to the high number of function evaluations (and simulations) required, these were discarded and are not discussed in the results.

It must be highlighted that, for some runs, the GB method stops due to an ending condition before the depletion of the budget of function calls N, converging to different local minima each time, with the resulting power density profiles shown in Fig. 5a. On the other hand, the SMGO-generated solutions shown in Fig. 5b are able to reproduce the target power density profile independently of the initial guess. Table 1 shows the mean, maximum, and minimum values of the root mean squared error $\varepsilon_r = \text{rms}(\breve{P}(s) - P(s, \boldsymbol{x}_r^{*\langle N \rangle}))$ of the resulting best profiles $P(s, \boldsymbol{x}_r^{*\langle N \rangle})$ with respect to the target profile for the optimization runs $r = 1, \ldots, 10$. It is noticed that the rms error of the SMGO solutions is one order of magnitude lower than that of the GB solutions.

B. DESIGN WITH EIGHT WINDINGS

The methodology is now applied to a setting with windings ($D = 16$). Again the performance of the SMGO solution is compared with that of a GB method. Eight independent optimization runs are carried out with GB and SMGO, given a budget of $N = 2500$ evaluations. Similar to the previous test case, the mean, minimum and maximum of the rms error ε_r across the runs are listed in Table 2. The solution found by SMGO is compared to the (pre-designed) target arrangement as shown in Fig. 6. Fig. 7a shows the power profiles found with the GB method. It is observed that the solutions follow the trend but they are not able to reproduce the details of the peaks. Fig. 7b shows the power profiles provided by SMGO, the solutions are much closer to the target profile, tracking some of the peaks. This high-dimensional test shows the capacity of the proposed methodology to achieve a satisfactory power profile, even with a large number of decision variables.

C. COIL DESIGN FROM ARBITRARY POWER DENSITY PROFILES

The proposed IH design methodology is used to achieve arbitrarily-designed power profiles as shown in Fig. 8 (red), including ramps, steps, peaks, discontinuities and non-smooth variations. In contrast to the situation in the previous subsection, all of these targets do not have *a priori* known optimal coil configuration. The optimization with SMGO is run with a budget of $N = 1000$ evaluations, however, convergence is generally achieved within 500 evaluations for all the tests. Table 3 lists, for each test, the rms error of the best solutions provided by SMGO. It can be mentioned that the resulting errors are similar to those observed in the tests of the previous subsection, even if the requested profiles are much more complex and there is not any guarantee of these being achievable by the model.

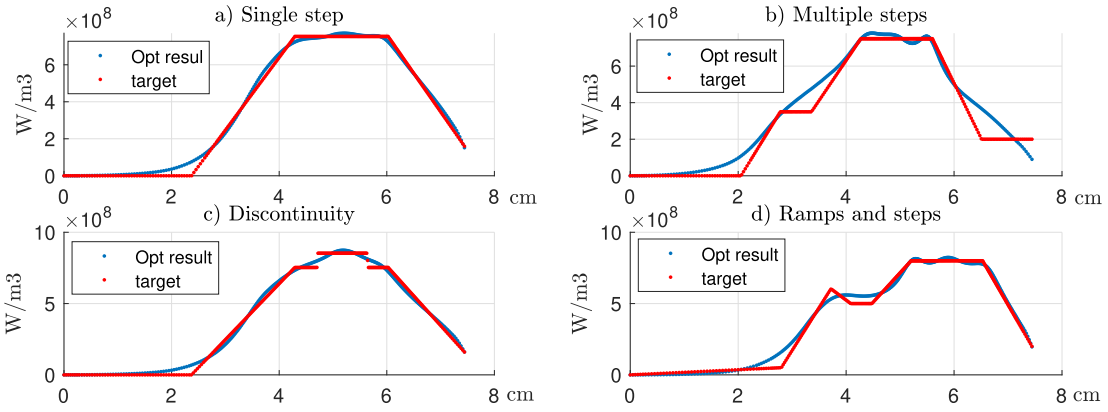

FIGURE 8. Fitting with different testing distributions with coefficient $\alpha = 0.025$ and $N_{max} = 1000$.

TABLE 3. Normalized rms errors for the design tests with target profiles in Fig. 8.

ine **Tested profile**	**RMS error**	**Tested profile**	**RMS error**
ine Single step	2.164E7	Multiple steps	5.629E7
ine Discontinuity	2.462E7	Ramps and step	3.119E7
ine			

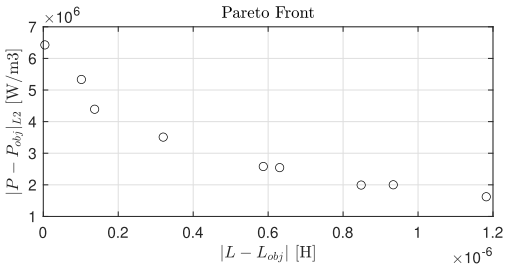

FIGURE 9. Points of the Pareto front obtained by each optimization with different weights w_l.

D. MULTI-OBJECTIVE PARETO FRONT

Finally, the methodology is exploited to find the Pareto front between two contrasting objectives, the achievement of a desired power density profile $\breve{P}(s)$, and the attainment of a target lumped-model equivalent inductance L_{eq}. For this test, we choose $\breve{P}(s)$ as the one in Fig. 8(d) composed of a series of ramps, while the inductance target is set to $\breve{L}_{eq} = 3\ \mu$H. The multi-objective problem in (10) is solved for increasing values of the parameter w_l. The results of the multi-objective SMGO problem are plotted in Fig. 9, where each point is the best solution for a different scalar parameter w_l. Clearly, the algorithm is able to provide multiple points of the Pareto front, providing a useful tool for the decision-making process in the design of IH systems.

V. CONCLUSION

The optimization of induction heating designs for generalized convex axisymmetric workpieces has been considered in this paper. To tackle such a problem, a novel parametrization based on the curvilinear abscissa on the heating surface was proposed, together with the use of SMGO, an efficient black-box optimization algorithm. The proposed parametrization methodology allows for a generalized optimization procedure which can be applied to complex convex-shaped surfaces. Furthermore, with the new parametrization, the resulting optimization problem allows to conveniently encode non-overlapping constraints among windings. Moreover, the SMGO black-box optimization algorithm has demonstrated its efficacy in solving the design problem involving a high number of windings. The methodology has been evaluated on a large set of problems of varying complexity, and close-to-optimal solutions have been found in all the situations, both for single and multi-objective design problems.

REFERENCES

[1] E. Rapoport and Y. Pleshivtseva, *Optimal Control of Induction Heating Processes*, 1st ed., Boca Raton, FL, USA: CRC Press, 2006, doi: 10.1201/9781420019490.

[2] A. Canova, G. Gruosso, and M. Repetto, "Magnetic design optimization and objective function approximation," *IEEE Trans. Magn.*, vol. 39, no. 5, pp. 2154–2162, Sep. 2003.

[3] P. Di Barba, F. Dughiero, M. Forzan, and E. Sieni, "A Paretian approach to optimal design with uncertainties: Application in induction heating," *IEEE Trans. Magn.*, vol. 50, no. 2, pp. 917–920, Feb. 2014.

[4] K. Gadó and T. Orosz, "Robust and multi-objective Pareto design of a solenoid," *Electronics*, vol. 10, no. 17, p. 2139, Sep. 2021.

[5] F. Grimaccia, G. Gruosso, M. Mussetta, A. Niccolai, and R. E. Zich, "Design of tubular permanent magnet generators for vehicle energy harvesting by means of social network optimization," *IEEE Trans. Ind. Electron.*, vol. 65, no. 2, pp. 1884–1892, Feb. 2018.

[6] P. Di Barba, M. E. Mognaschi, D. A. Lowther, and J. K. Sykulski, "A benchmark TEAM problem for multi-objective Pareto optimization of electromagnetic devices," *IEEE Trans. Magn.*, vol. 54, no. 3, pp. 1–4, Mar. 2018.

[7] P. Di Barba, A. Savini, F. Dughiero, and S. Lupi, "Optimal shape design of devices and systems for induction-heating: Methodologies and applications," *COMPEL-Int. J. Comput. Math. Electr. Electron. Eng.*, vol. 22, no. 1, pp. 111–122, Mar. 2003.

[8] Y. Pleshivtseva, P. D. Barba, E. Rapoport, B. Nacke, A. Nikanorov, S. Lupi, E. Sieni, and M. Forzan, "Multi-objective optimisation of induction heaters design based on numerical coupled field analysis," *Int. J. Microstructure Mater. Properties*, vol. 9, no. 6, p. 532, 2014.

[9] Y. Gu, J. Xu, and T. Fu, "Design and optimization of coil structure based on the uniformity of core temperature field," *J. Mech. Sci. Technol.*, vol. 36, no. 6, pp. 2903–2912, Jun. 2022, doi: 10.1007/s12206-022-0522-y.

[10] Y. Pleshivtseva, E. Rapoport, B. Nacke, A. Nikanorov, P. Di Barba, M. Forzan, S. Lupi, and E. Sieni, "Design concepts of induction mass heating technology based on multiple-criteria optimization," *COMPEL-Int. J. for Comput. Math. Electr. Electron. Eng.*, vol. 36, no. 2, pp. 386–400, Mar. 2017.
[11] D. Y. Um, M. J. Kim, S. A. Chae, and G. S. Park, "Investigation of dual coil induction heating for enhanced temperature distribution optimization," *IEEE Access*, vol. 12, pp. 37129–37140, 2024.
[12] *TEAM*. Accessed: Jan. 2024. [Online]. Available: https://www.compumag.org/wp/team
[13] J. D. Martin, "Exploring additive manufacturing processes for direct 3D printing of copper induction coils," in *Proc. ASME Int. Mech. Eng. Congr. Expo.*, Nov. 2017, pp. 1–7, doi: 10.1115/imece2017-71685.
[14] E. Spateri, F. Ruiz, and G. Gruosso, "Modelling and simulation of quasi-resonant inverter for induction heating under variable load," *Electronics*, vol. 12, no. 3, p. 753, Feb. 2023.
[15] R. M. Baker, "Classical heat flow problems applied to induction billet heating," *Trans. Amer. Inst. Electr. Eng., II, Appl. Ind.*, vol. 77, no. 2, pp. 106–112, May 1958.
[16] P. Karban, D. Pánek, T. Orosz, and I. Doležel, "Semi-analytical solution for a multi-objective TEAM benchmark problem," 2020, *arXiv:2008.06954*.
[17] K. J. Binns, P. J. Lawrenson, and C. Trowbridge, *The Analytical and Numerical Solution of Electric and Magnetic Fields*. New York, NY, USA: Wiley, 1992.
[18] O. U. Rehman, S. Yang, S. Khan, and S. U. Rehman, "A quantum particle swarm optimizer with enhanced strategy for global optimization of electromagnetic devices," *IEEE Trans. Magn.*, vol. 55, no. 8, pp. 1–4, Aug. 2019.
[19] S. Tu, O. U. Rehman, S. U. Rehman, S. Ullah, M. Waqas, and R. Zhu, "A novel quantum inspired particle swarm optimization algorithm for electromagnetic applications," *IEEE Access*, vol. 8, pp. 21909–21916, 2020.
[20] L. Sabug, F. Ruiz, and L. Fagiano, "SMGO: A set membership approach to data-driven global optimization," *Automatica*, vol. 133, Nov. 2021, Art. no. 109890.
[21] L. Sabug, F. Ruiz, and L. Fagiano, "SMGO-Δ: Balancing caution and reward in global optimization with black-box constraints," *Inf. Sci.*, vol. 605, pp. 15–42, Aug. 2022.
[22] COMSOL AB. *COMSOL Multiphysics*. Accessed: Jan. 2024. [Online]. Available: www.comsol.com
[23] G. Paoli, O. Biro, and G. Buchgraber, "Complex representation in nonlinear time harmonic eddy current problems," *IEEE Trans. Magn.*, vol. 34, no. 5, pp. 2625–2628, Sep. 1998.

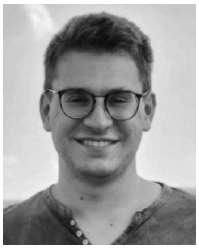

ENRICO SPATERI (Graduate Student Member, IEEE) was born in Milan, Italy. He received the bachelor's degree in engineering physics and the M.Sc. degree in automation and control engineering from Politecnico di Milano, Italy, in 2018 and 2021, respectively. He is currently pursuing the Ph.D. degree in electrical engineering. His research interests include analysis, reduced order modeling, and optimization for electro-thermal and electromagnetic-thermal coupled problems and applications, including thermoforming, induction heating, and induction thermography.

LORENZO SABUG JR. received the M.Sc. degree in electrical engineering from RWTH Aachen University, Germany, in 2016, and the Ph.D. degree in information technology (systems and control) from Politecnico di Milano, Milan, Italy, in 2023. From 2016 to 2019, he was a Research Associate with the University of the Philippines Diliman, where he led the development of a communications payload for the Philippine microsatellite Diwata-2, launched in 2018. He is currently a Postdoctoral Researcher with Politecnico di Milano, where he works on novel data-driven optimization methods and their industrial and aerospace applications.

FREDY RUIZ (Senior Member, IEEE) was born in Facatativá, Colombia. He received the bachelor's and M.Sc. degrees in electronics engineering from Pontificia Universidad Javeriana, Colombia, in 2002 and 2006, and the Ph.D. degree in computer and control engineering from Politecnico di Torino, Italy, in 2009. From 2010 to 2014, he was an Assistant Professor and an Associate Professor with Pontificia Universidad Javeriana, from 2015 to 2019, where he was also the Head of the Electronics Engineering Department, from 2014 to 2016. He was a Fulbright Visiting Scholar with the University of California at Berkeley, in 2013, and a Visiting Professor with Politecnico di Torino, in 2018. He is currently an Associate Professor with Politecnico di Milano, Italy. His research interests include control and optimization, in particular, the use of data-driven techniques in optimal estimation and controller design, with applications in smart grids, power electronics, robotics, and biotechnology. He works also on the design of demand-side management strategies for the smart grid.

GIAMBATTISTA GRUOSSO (Senior Member, IEEE) was born in 1973. He received the M.S. and Ph.D. degrees in electrical engineering from Politecnico di Torino, Italy, in 1999 and 2003, respectively. From 2002 to 2011, he was an Assistant Professor with the Department of Electronics and Informatics, Politecnico di Milano. He has been an Associate Professor with the Department of Electronics and Informatics, Politecnico di Milano, since 2011. He is currently the Head of the Simlab40 Group, Politecnico di Milano. He is the author of more than 80 papers in journals and conferences on the topics. He does research in electrical engineering, electronic engineering, and industrial engineering. His main research interests include electrical vehicle transportation electrification, electrical power systems optimization, simulation of electrical systems, digital twins for smart mobility, factory and city, and how they can be obtained from data.

Open Access funding provided by 'Politecnico di Milano' within the CRUI CARE Agreement